Electronic structure of $SrFe^{4+}O_3$ and related Fe perovskite oxides

A. E. Bocquet*
Department of Applied Physics, University of Tokyo, Bunkyo-ku, Tokyo 113, Japan

A. Fujimori,† T. Mizokawa, T. Saitoh, and H. Namatame
Department of Physics, University of Tokyo, Bunkyo-ku, Tokyo 113, Japan

S. Suga
Department of Material Physics, Faculty of Engineering Science, Osaka University, Toyonaka, Osaka 560, Japan

N. Kimizuka
National Institute for Research in Inorganic Materials, Namiki, Tsukuba-shi, Ibaraki 305, Japan

Y. Takeda
Department of Chemistry, Faculty of Engineering, Mie University, Tsu 514, Japan

M. Takano
Institute for Chemical Research, Kyoto University, Uji, Kyoto 611, Japan
(Received 11 March 1991; revised manuscript received 16 September 1991)

The electronic structure of $SrFeO_3$ has been investigated by x-ray photoemission and ultraviolet photoemission spectroscopy. We find that the ground state consists of heavily mixed d^4 and $d^5\underline{L}$ states, reflecting the large covalency. The Fe 3*s* core-level splitting, together with a subsequent cluster-model configuration-interaction calculation, shows that a high-spin $t_{2g}^3e_g$ ground state is stabilized. The Fe 2*p* core levels have been interpreted using a *p-d* charge-transfer cluster-model calculation. The charge-transfer energy $\Delta_{\rm eff}$, defined with respect to the lowest multiplet levels of the d^4 and $d^5\underline{L}$ configurations, is negative, which means that a large amount of charge is transferred via Fe—O bonds from the O 2*p* bands to the metal *d* orbitals and that the ground state is dominated by the $d^5\underline{L}$ configuration. This reduces the charge on the ionic sites, leading to only a small chemical shift between the Fe^{3+} and Fe^{4+} compounds. The band-gap energy $E_{\rm gap}$, calculated using the cluster model for the high-spin d^4 configuration, is small due to the small charge-transfer energy and the large exchange stabilization of the adjacent d^5 configuration. This small value for $E_{\rm gap}$ leads to the presence of itinerant *d* electrons in the periodic lattice, causing metallic conductivity in $SrFeO_3$ and charge disproportionation in $CaFeO_3$.

I. INTRODUCTION

Stimulated by the recent discovery of high-temperature superconductivity in copper oxides[1] and by a reinterpretation of photoemission spectroscopy data,[2] interest has been revived in the condensed-matter physics community in a fuller understanding of the 3*d* transition-metal (TM) oxides. Much work has been done on simple divalent TM oxides, such as MnO, NiO, and CoO,[3–5] which has shown that the band gaps of the insulating oxides of the late transmission metals are of a ligand-to-metal charge-transfer type, defined by a charge-transfer energy Δ, where $\Delta < U$, the on-site *d-d* Coulomb correlation energy. Perovskite oxides (AMO_3), in which the transition-metal cation (M) is coordinated octahedrally to six oxygen ligands, have also been studied[6,7] as they have a relatively simple structure and allow the 3*d* transition metals to be stabilized in unusually high valence states. For the TM perovskite oxides, an increase in formal valency will increase the covalency of the M—O bond, thereby increasing the importance of the O 2*p* bands on the electronic states. Thus it is expected that their electronic structure will be greatly dependent on hybridization effects between the highly correlated TM 3*d* levels and the band-like O 2*p* levels.

The cubic perovskite $SrFeO_3$, in which iron is present as Fe^{4+}, is interesting due to its unusual magnetic and electronic properties. $SrFeO_3$ retains its cubic structure and a metallic conductivity of $\approx 10^{-3}$ Ω cm down to 4 K,[8] in contrast to trivalent $LaFeO_3$, which is an antiferromagnetic insulator. According to ligand field theory, four 3*d* electrons in an octahedral crystal field can assume either a high-spin $t_{2g}^3e_g$ configuration or a low-spin t_{2g}^4 configuration, with the latter configuration being stabilized when the crystal field splitting, $10Dq$, is large. The magnitude of the magnetic moment has been measured by neutron scattering by Takeda, Komura, and Watanabe[9] as $\mu_{Fe^{4+}} = 3.1\mu_B$ in the screw antiferromagnetic state below $T_N \approx 134$ K,[10] suggesting that $SrFeO_3$ is high spin with three electrons filling the t_{2g} band, and the remaining e_g electron itinerant. It has been proposed that these itinerant *d* electrons are accommodated in a broad σ^* band formed between the metal e_g orbitals and the O 2*p* bands, giving rise to metallic conductivity.[9,11]

This may explain the absence of any Jahn-Teller distortion that would be expected for a localized d^4 system. Mössbauer spectroscopy (MS) studies, based on the behavior of doped $La_{1-x}Sr_xFeO_3$ $(0.1<x<0.6)$,[12] also indicate a high-spin state for $SrFeO_3$. For $La_{1-x}Sr_xFeO_3$ and $CaFeO_3$, which are semiconductors below room temperature, the single set of Fe^{4+} magnetic hyperfine patterns in the Mössbauer emission at room temperature splits into two distinct patterns at low temperature. Thus a charge disproportionation due to the localization of the itinerant electrons at alternating Fe^{3+} and Fe^{5+} sites has been proposed for these compounds.[13]

In this work, the electronic structure of $SrFeO_3$ has been studied by core-level and valence-band x-ray photoemission (XPS) and ultraviolet photoemission (UPS) spectroscopy. Results for the perovskites $LaFe^{3+}O_3$ and $YFe^{3+}O_3$, as well as for α-$Fe_2^{3+}O_3$ which has an α-corundum structure also with Fe coordinated octahedrally to six O atoms, have been included for comparative purposes. The Fe $3s$ core levels show that $SrFeO_3$ is high spin in the ground state, in agreement with a subsequent cluster-model configuration-interaction calculation. An examination of the Fe $2p$ and O $1s$ levels confirms that hybridization and correlation effects indeed play a central role in the electronic structure, with the ground state consisting of heavily mixed d^4 and $d^5\underline{L}$ states with the latter being predominant, where $\underline{L}$ indicates an O $2p$ hole. Increased covalency in the Fe^{4+} compound results in a negligible chemical shift in the core levels between the Fe^{3+} and Fe^{4+} compounds.

II. EXPERIMENTAL PROCEDURE

Stoichiometric $SrFeO_3$ was prepared as follows. By heating a mixture of appropriate molar quantities of $SrCO_3$ and α-Fe_2O_3 in air at 1473 K, an oxygen deficient material $SrFeO_{3-\delta}$ was first obtained. A gold capsule charged with the oxygen deficient material and an oxygen supplier, $KClO_4$, was then pressed and heated at 1323 K under a pressure of 6 GPa for 30 min using a belt-type high-pressure apparatus. The final product was characterized by x-ray diffraction (XRD) and MS. A cubic perovskite structure was found with $a=0.3852$ nm. Good sample quality was assured by the ME spectrum at 4 K which consisted of a single Fe^{4+} magnetic hyperfine pattern. The spectrum did not show any Fe^{3+} components, such as those previously detected in measurements of nonstoichiometric $SrFeO_{2.97}$,[14] assuring that the oxygen deficiency of the present sample is much less than 1%. The $LaFeO_3$ and $YFeO_3$ samples were prepared by mixing appropriate molar quantities of Fe_2O_3 and either La_2O_3 or Y_2O_3 and firing in air at 1643 K for one week. Samples were confirmed to be single phase by XRD. The preparation of the Fe_2O_3 single crystal has been described previously.[15]

XPS measurements were carried out using a spectrometer equipped with a Mg $K\alpha$ source ($h\nu=1253.6$ eV), a He discharge lamp and a double-pass cylindrical mirror analyzer with a resolution of ≈ 1 eV for XPS and ≈ 0.2 eV for UPS. UPS spectra were obtained using He II radiation ($h\nu=40.8$ eV). Some measurements were also performed separately on an instrument equipped with an Al $K\alpha$ source ($h\nu=1486.6$ eV). All XPS spectra have been corrected for satellites arising from the x-ray source. The base pressure was $\approx 1\times 10^{-10}$ and all spectra were recorded at liquid-nitrogen temperatures (77 K) to prevent the removal of oxygen from the surface under ultrahigh-vacuum (UHV) conditions. Clean surfaces were obtained by scraping the sample *in situ* with a diamond file until the C $1s$ emission at ≈ 285 eV was negligibly small. Although no charging effects were observed for $SrFeO_3$, significant charging shifts were detected for the insulating compounds. For these compounds, calibration was performed by monitoring the binding energy of "adventitious" graphitic carbon, which is known to be 284.8 eV.

For the $LaFeO_3$ and $YFeO_3$ sintered samples, filing was successful in substantially reducing the O $1s$ emission located near 531.0 eV, which is normally associated with contaminants on the surface. However, some small emission invariably remained for $SrFeO_3$, even after repeated scraping. Furthermore, initial calculations of atomic concentrations within the sample using the core-level intensities and corresponding standard sensitivity factors[16] found an excess of O and Sr with respect to Fe. Figure 1 shows the O $1s$ and Sr $3d$ levels for $SrFeO_3$, with the O $1s$ peak resolved by a Gaussian and Lorentzian stripping routine into two components separated by 2.5 eV. One possible origin for the peak at around 530.2 eV may be contaminants present on the surface or in grain boundaries of the sintered samples, detected due to the great

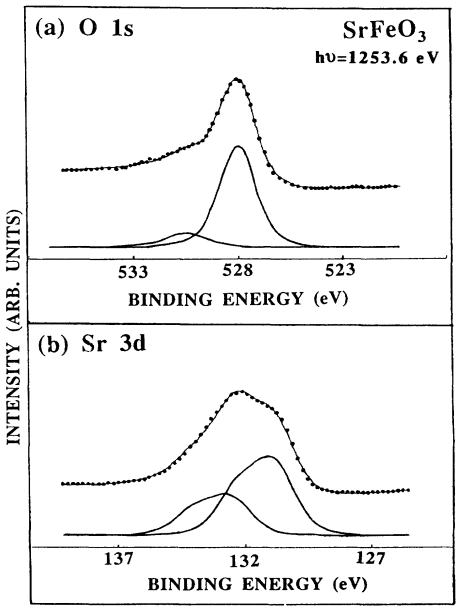

FIG. 1. O $1s$ and Sr $3d$ core levels for $SrFeO_3$. Peaks were resolved using a Gaussian and Lorentzian stripping routine. The higher binding-energy peaks in both spectra arise due to the presence of minor phases on the surface or in grain boundaries.

surface sensitivity of the photoemission technique. An analysis of the Sr 3*d* peak also shows it can be resolved into two spin-orbit doublets [Fig. 1(b)] separated by 1.7 eV, which do not change upon filing. The higher-energy component occurs at a binding energy typical of SrO.[17] This suggests that the extraneous peaks in the O 1*s* and Sr 3*d* levels may arise from the presence of a minor phase, most probably SrO in the surface layers or in grain boundaries. After removing the contributions from these extra components, we arrive at the correct atomic concentrations of 1:1:3 for $SrFeO_3$. The presence of these minor phases is, however, unlikely to influence the Fe core-level spectra and the electronic structure of the bulk material deduced from these spectra, which we are mainly concerned with in the present work.

III. RESULTS AND DISCUSSION

Binding-energy data for the core-level peaks of $SrFeO_3$, $LaFeO_3$, $YFeO_3$, Fe_2O_3, and Fe_xO[18] are summarized in Table I.

A. Fe 3*s* core levels

An accurate measurement of the magnetic moment can give much information on the electronic structure. Much work has been done by Mössbauer effect, magnetization, and neutron diffraction techniques on $SrFeO_3$,[9–14,19] with unfortunately many inconsistent results being obtained, leading to confusion regarding the nature of the 3*d* electrons. These conflicting results may be traced back to the great sensitivity of the magnetic properties to the oxygen substoichiometry. One microscopic probe of the local moment is the splitting observed in the 3*s* and 2*s* core-level photoemission spectra of magnetic TM ions.[20] The primary, but not exclusive[21,22] mechanism responsible for the splitting of these levels is believed to be the exchange interaction between the *s* core hole spin and the 3*d* spin, which leads to an energy difference between photoemission final states with the remaining *s* electron parallel, or antiparallel, to the 3*d* spin. Although an extensive collection of Fe 3*s* data by van Acker *et al.*[22] has shown that other interactions, such as the core-valence and valence-valence Coulomb interactions, must be important especially for metals and alloys, gross general trends among oxides seem to be consistent with this mechanism. That is, the 3*s* splittings will be roughly proportional to

$$(2S+1)E(\underline{s},d)\ , \tag{1}$$

where S is the magnitude of the local 3*d* spin, and $E(\underline{s},d)$ is the exchange integral between the $\underline{s}$ core hole and the 3*d* electron.

In Fig. 2, the Fe 3*s* core-level region for $SrFeO_3$ is compared with those for $YFeO_3$ and Fe_2O_3, which have simple high-spin $(d^5)^6S$ configurations in the ground state. (Data for $LaFeO_3$ are not shown as the La 4*d* peak partially obscures the 3*s* doublet.) Although, due to the complex interactions involved, the absolute magnitudes of the 3*s* splittings are of little value, the ratio of the splitting between the ^5S and ^7S states in the d^5 compounds compared to the splitting for $SrFeO_3$ should give some information on the local magnetic moment. This ratio falls in the range 1.2–1.1, consistent with a value of $[2\times(5/2)+1]/[2\times(4/2)+1]=1.2$ expected for $SrFeO_3$ in a high-spin configuration. As will be shown below, the Fe core-level main peaks are due to ligand-to-metal 3*d* charge-transfer screened final stated $\underline{c}d^{n+1}\underline{L}$, and there-

TABLE I. Binding energies and splittings (in eV) for XPS core-level main peaks.

Core level	$SrFeO_3$	$LaFeO_3$	$YFeO_3$	Fe_2O_3	Fe_xO[a]
Fe 3*s* (^{2S+2}S)	92.4	93.0	92.8	94.2	
Fe 3*s* splitting	5.5		6.7	6.2	
Fe $2p_{3/2}$	709.3	709.4	709.7	711.2	709.2
O 1*s*	528.1[b]	528.7	529.0	530.2	530.0
O 1*s*–Fe 2*p* splitting	181.2	180.7	180.7	181.0	179.2
Sr $3d_{5/2}$	131.4[b]				
La $3d_{5/2}$		833.3			
Y $3d_{5/2}$			156.4		

[a]Reference 18.
[b]Main component data.

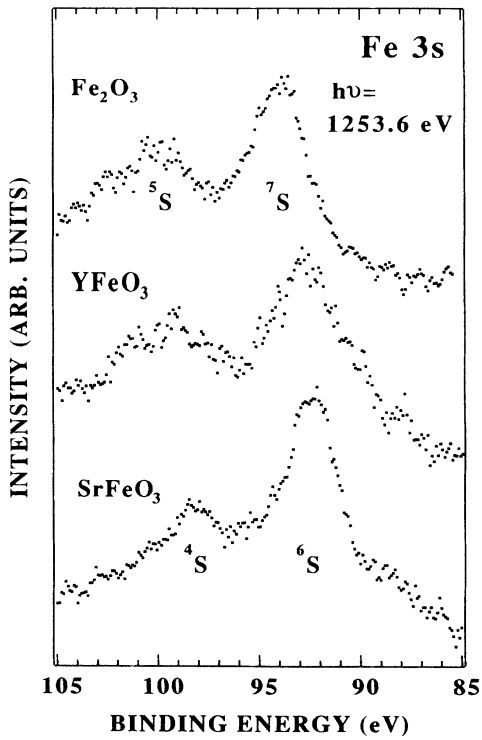

FIG. 2. Fe 3*s* core-level XPS spectra for Fe_2O_3, $YFeO_3$, and $SrFeO_3$. The peaks of the d^5 compounds are split into ^5S and ^7S final states, while that of d^4 $SrFeO_3$ is split into ^4S and ^6S final states. The peak splittings are 6.2, 6.7, and 5.5 eV, respectively.

fore such a simple analysis is not strictly valid. However, we expect a more thorough analysis would lead to a similar conclusion as the screening occurs predominantly via transfer of an electron with a spin antiparallel to that of the d electrons in either the d^4 or d^5 configurations, leading to a similar splitting ratio.

We have applied a cluster-model configuration-interaction calculation, including hybridization effects, to an $(FeO_6)^{8-}$ octahedron in order to study the stability of various configurations in the ground state. According to ligand field theory, the ground state of the d^4 system in an octahedral crystal field can be stabilized as either a low-spin $^3T_1$ triplet or a high-spin ^5E quintuplet, depending on the magnitude of $10Dq$. Increase in covalency resulting from a decrease in Δ should increase $10Dq$, stabilizing a low-spin state. We shall investigate this point using the cluster model in the case of small (or negative) Δ, where the basic assumption of ligand field theory that the strength of the p-d hybridization is constant throughout the d^4 multiplet may break down. For both the $^3T_1$ and ^5E symmetries, we have described the ground state of the cluster as a hybridized state between the purely ionic $Fe^{4+}(O^{2-})_6$ configuration, and states screened by O $2p \rightarrow$ Fe $3d$ charge transfer:

$$\Psi_g(^3T_1 \text{ or } ^5E) = a|d^4(^3T_1 \text{ or } ^5E)\rangle + b|d^5\underline{L}(^3T_1 \text{ or } ^5E)\rangle + \cdots , \quad (2)$$

where $\underline{L}$ describes a ligand hole. On the right-hand side of Eq. (2), we have implicitly assumed summation over $\underline{L}_{\sigma\uparrow\downarrow}$ and $\underline{L}_{\pi\uparrow}$. The Coulomb interaction terms for the d^4 ionic basis states have been tabulated in terms of the A, B, and C Racah parameters by Sugano, Tanabe, and Kanimura.[23] For the triplet state, various nondegenerate d^4 configurations are allowed by symmetry. The screened basis states $d^5\underline{L}$ were approximated by single Slater determinants. The diagonal matrix elements of H for these basis sets were expressed in terms of the parameters u, u', and j, originally proposed by Kanamori,[24] where $u = \langle \xi\xi|H|\xi\xi\rangle$, the Coulomb interaction between d electrons in the same orbit, $u' = \langle \xi\eta|H|\xi\eta\rangle$, the Coulomb interaction between d electrons in different orbits and $j = \langle \xi\eta|H|\eta\xi\rangle$, the exchange interaction. The off-diagonal matrix elements between the d^4 and $d^5\underline{L}$ bases, etc., were expressed by a hybridization term T, with any off-diagonal matrix elements for the Coulomb and exchange interactions neglected. Racah parameters, B and C, for the Fe^{4+} ion were interpolated from values for Fe^{3+} and Fe^{5+} (Ref. 25). The ligand-to-metal charge-transfer energy Δ is simply defined as

$$\Delta = E(d^{n+1}\underline{L}) - E(d^n) , \quad (3)$$

where $E(d^n)$ denotes the center of gravity of the d^n multiplet. We have assumed $T_\sigma = \sqrt{3}(pd\sigma)$ and $T_\pi = 2(pd\pi)$ with $T_\pi \approx -0.5T_\sigma$ as before.[4] The charge-transfer energy Δ and the transfer integral T_σ were treated as adjustable parameters, with all other parameters listed in more detail in Table II.

Results using the above model for particular values of the hybridization are displayed in Fig. 3. We have found that for all reasonable values of Δ and T, the high-spin configuration is stable. This is primarily due to the large exchange stabilization of the $d^5(^6A_{1g})\underline{L}$ configuration, which lowers the energy of the high-spin d^4 state through hybridization. That is, the inherent stability of the half closed-shell $d^5\underline{L}$ configuration leads to the stabilization of the d^4 high-spin state through hybridization effects. We find that the triplet state will only be stable for very large values of T. If we include $10Dq$ contributions of the order of ≈ 0.5 eV arising from the nonorthogonality between the Fe $3d$ and O $2p$ orbitals,[26] the energy of the low-spin configuration will then be lowered by this amount, but the high-spin configuration would still remain the ground state. This result is in agreement with a recent cluster calculation using the discrete-variational $X\alpha$ method of Adachi and Takano,[27] in which it was found that the up-spin antibonding Fe $3d$ orbitals were occupied, while the down-spin orbitals were empty, indicating a high-spin state.

B. Fe $2p$ and O $1s$ core levels

The Fe $2p$ core-level regions for Fe_2O_3, $LaFeO_3$, and $SrFeO_3$ are shown in Fig. 4. Results for $YFeO_3$ were almost identical to those for $LaFeO_3$, which were consistent with previous studies.[6] Only small differences in the core-level binding energies are observed between perovskite-type $LaFeO_3$ and $SrFeO_3$, but a rigid shift of ≈ 2 eV for all core levels and the top of the valence band

TABLE II. Basis functions, Hamiltonians, and parameters for the ^5E and $^3T_1$ symmetries for the ground state of an $(FeO_6)^{8-}$ cluster. Only those corresponding to the lowest energy ionic state (d^4 configuration) and its one hole screening states ($d^5\underline{L}$ configuration) are listed. B and C values for Fe^{4+} were interpolated from those in Ref. 25. $E(d^n)$ is the center of gravity of the d^n multiplet. $\Delta = E(d^5\underline{L}) - E(d^4)$ is the ligand-to-metal charge-transfer energy.

^5E symmetry	
$\phi_1 = \lvert t_{2\uparrow}^3 e_\uparrow(^5E)\rangle$	$H_{1,1} = 6u' - 6j - E(d^4)$
$\phi_2 = \lvert t_{2\uparrow}^3 t_{2\downarrow} e_\uparrow \underline{L}_{\pi\uparrow}\rangle$	$H_{2,2} = u + 9u' - 6j - E(d^5) + \Delta$
$\phi_3 = \lvert t_{2\uparrow}^3 e_\uparrow^2 \underline{L}_{\sigma\downarrow}\rangle$	$H_{3,3} = 10u' - 10j - E(d^5) + \Delta$
$\phi_4 = \lvert t_{2\uparrow}^3 e_\uparrow e_\downarrow \underline{L}_{\sigma\uparrow}\rangle$	$H_{4,4} = 0.5u + 9.5u' - 6j - E(d^5) + \Delta$
$H_{1,2} = \sqrt{3}T_\pi$, $H_{1,3} = T_\sigma$, $H_{1,4} = \sqrt{2}T_\sigma$	
$^3T_1$ symmetry	
$\phi_{1-7} = \lvert t_{2\uparrow}^3 t_{2\downarrow}(^3T_1)\rangle$, etc.[a]	
$\phi_8 = \lvert t_{2\uparrow}^3 t_{2\downarrow}^2 \underline{L}_{\pi\uparrow}\rangle$	$H_{8,8} = 2u + 8u' - 4j - E(d^5) + \Delta$
$\phi_9 = \lvert t_{2\uparrow}^3 t_{2\downarrow} e_\uparrow \underline{L}_{\sigma\downarrow}\rangle$	$H_{9,9} = u + 9u' - 6j - E(d^5) + \Delta$
$\phi_{10} = \lvert t_{2\uparrow}^3 t_{2\downarrow} e_\downarrow \underline{L}_{\sigma\uparrow}\rangle$	$H_{10,10} = 2u + 8u' - 4j - E(d^5) + \Delta$
$H_{1,8} = \sqrt{2}T_\pi$, $H_{1,9} = \sqrt{2}T_\sigma$, $H_{1,10} = \sqrt{2}T_\sigma$	
Parameters	
$T_\pi = 2(pd\pi)$, $T_\sigma = \sqrt{3}(pd\sigma)$	
$u = A + 4B + 3C$, $u' = A - B + C$, $j = 2\frac{1}{2}B + C$	
$E(d^n) = \frac{1}{2}n(n-1)[A - \frac{14}{9}B + \frac{7}{9}C]$	

[a]Energies for the seven ionic basis functions allowed by symmetry are taken from tables listed in Ref. 23.

is observed for Fe_2O_3. Fe_2O_3 is a n-type semiconductor, in which the valence-band maximum is located well below the Fermi level, while $LaFeO_3$ is a p-type semiconductor and $SrFeO_3$ is a metal.

Strong core-level satellites are observed in the Fe $2p$ spectra for Fe_2O_3 and $LaFeO_3$, with an apparently weaker satellite present for $SrFeO_3$. These satellites have been shown to be associated with screening of the Fe $3d$ orbitals at the core hole site.[15] Similar but weaker satellites are also observed for the Fe $3p$ levels (not shown), appearing at a similar binding energy separation. Fujimori *et al.*[15] have suggested that the main lines of the Fe_2O_3 Fe core levels may be due to $L \rightarrow d$ well screened $\underline{c}3d^6\underline{L}$ states whereas the satellites are poorly screened $\underline{c}3d^5$ states, in accordance with earlier work by Veal and Paulikas.[28]

It has been shown[5,15,29] that much useful information, such as the on-site d-d Coulomb interaction, U, and the ligand-to-metal charge-transfer energy Δ, can be obtained from correct modeling of the intensities and positions of the XPS $2p$ core-level satellites. Recently, Park *et al.*[29] have presented a charge-transfer model for the late TM dihalides based on earlier work by van der Laan *et al.*,[30] where the XPS $2p$ core-level spectrum was described by a cluster-type configuration-interaction Hamiltonian, with the d-d Coulomb repulsion U, the core-hole–d-electron Coulomb interaction Q, the charge-transfer energy Δ, and the ligand $2p$-metal $3d$ hybridization T as parameters. We have extended this model to investigate the $Fe^{3+}(d^5)$ and $Fe^{4+}(d^4)$ $2p$ core-levels, where a high-spin configuration has been assumed for both cases. As the model will be described in more detail in a subsequent publication,[31] only a brief outline will be presented here.

The ground state is described as in Eq. (2) as a mixture of the purely ionic state $|d^n\rangle$ and screened charge-transfer states $|d^{(n+m)}\underline{L}^m\rangle$ in which one or more electrons are transferred to the $3d$ levels from neighboring ligand O $2p$ orbitals:

$$\Psi_g = a_0|d^n\rangle + \sum_m a_m|d^{(n+m)}\underline{L}^m\rangle \ . \tag{4}$$

Here $n=4$ or 5 and the right-hand side is summed over the number of $\underline{L}$ ligand holes $m=1,2,\ldots,10-n$. Crystal-field effects and the exchange interaction are introduced by extending the basis set to discriminate between the $t_{2g\uparrow\downarrow}$ and $e_{g\uparrow\downarrow}$ symmetry states. For the

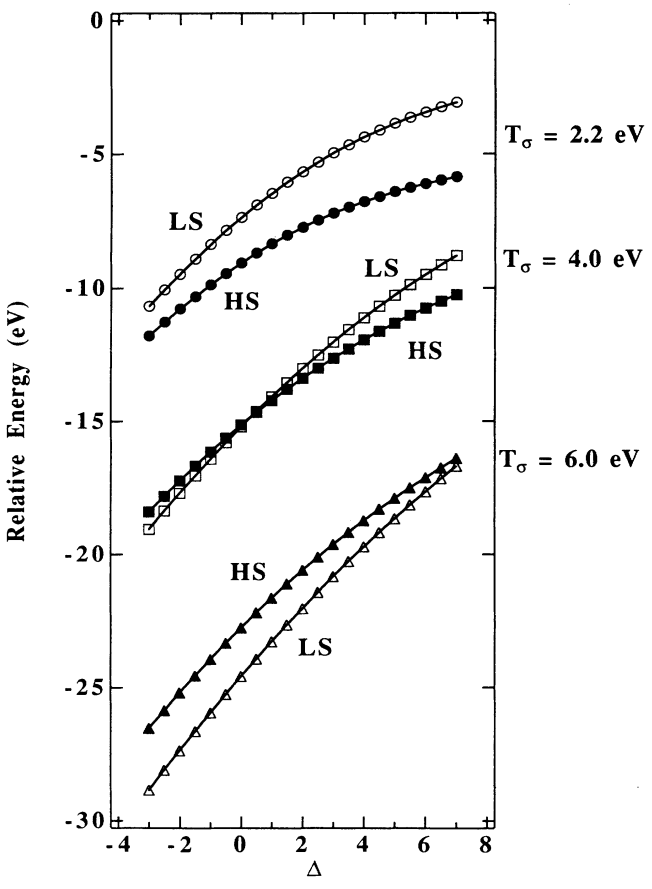

FIG. 3. Energy curves as a function of Δ for various values of the hybridization, T_σ, from a configuration-interaction calculation of the ground state of an $(Fe^{4+}O_6)^{8-}$ cluster. Open markers indicate stabilization energies for the low-spin (LS) $^3T_1$ triplet and closed markers the high-spin (HS) ^5E quintuplet. We find that the HS state is stabilized for all reasonable values of Δ and T_σ. The LS is only stable for unreasonably large values of T_σ. The zero energy is set to the center of gravity of the d^4 configuration.

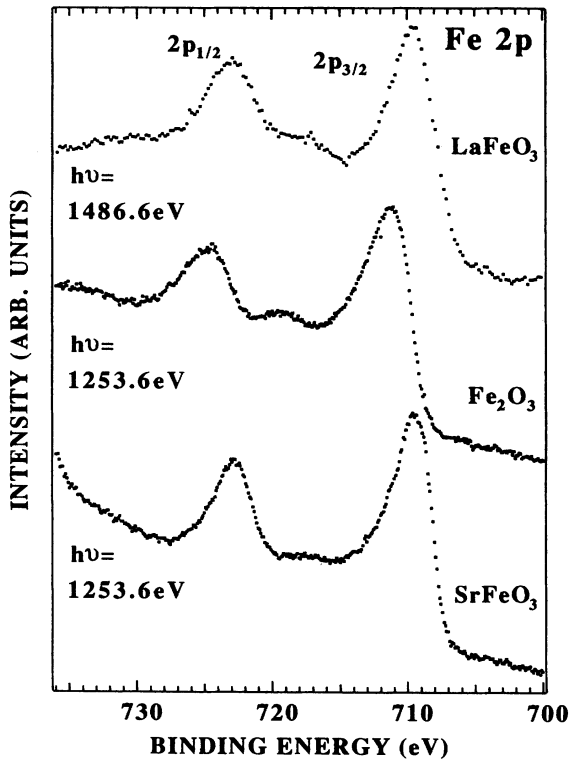

FIG. 4. Fe $2p$ core-level XPS spectra for Fe_2O_3, $LaFeO_3$, and $SrFeO_3$. Strong satellite features are observed for the d^5 compounds with an apparently weaker satellite present for $SrFeO_3$.

$^6A_{1g}(d^5)$ configuration we have 12 basis states and for $^5E_g(d^4)$ we have 24. The diagonal matrix elements of the Hamiltonian for each configuration were given by the aforementioned Kanamori parameters, and additional charge-transfer and *d-d* Coulomb interaction energies were added to the screened states due to the presence of the screening electrons. The matrix element of the ionic basis state, $E(d^n)$, was set to zero as a reference point. Hybridization between the ligand 2*p* and metal 3*d* levels was included via the one-electron mixing matrix element, T, where $T_\sigma=\sqrt{3}(pd\sigma)$, $T_\pi=2(pd\pi)$, and we have assumed $T_\pi\approx-0.5T_\sigma$ as before. The eigenfunctions for the ground state are found by diagonalization of the Hamiltonian matrix. The XPS final states will differ from the ground state by the attraction between the photoionization core hole and the 3*d* electron, Q, which pulls down the 3*d* levels. We have neglected the exchange interaction between the core hole and the *d* electrons, and have assumed the relationship $U/Q\approx0.83$. After finding the eigenfunctions of the final state matrix, the XPS spectrum can be calculated in the sudden approximation in the usual way.[29] The inclusion of the *d-d* exchange interaction (represented by the Kanamori parameters u, u', and j) and the anisotropic hybridization ($T_\sigma\neq T_\pi$) was essential to reproduce the experimental spectra using reasonable values for the parameters. The reader is referred to Ref. 29 for more detail.

Using this model, we have obtained calculated spectra for d^5 and d^4 high-spin configurations. The parameters U, Δ, and T_σ were varied to provide a best fit to experimental data for $LaFeO_3$ and $SrFeO_3$. Excellent agreement between theory and experiment was obtained, as is shown in Fig. 5. The best-fit parameters are listed in Table III. The subtraction of the secondary electron background was a nontrivial problem, since the parameter values are dependent on the height of the subtracted background. Proportional coefficients for the integral background were determined from those core levels which show no charge-transfer satellites, such as Sr 3*d* or La 3*d*, and integral backgrounds determined from these coefficients were then subtracted from the Fe 2*p* core-level spectra. (The large intensity at ≈30 eV in the $SrFeO_3$ spectrum, which partially obscures the satellite of the $2p_{1/2}$ peak, is due to O *KLL* Auger emission found at this binding energy for Mg $K\alpha$ radiation.)

Using parameter values based on those found earlier in valence-band studies of Fe_2O_3,[15] we were able to successfully model the Fe 2*p* spectra of $LaFeO_3$ and Fe_2O_3 (not shown). As indicated in the figure, the spectra consist of a main spin-orbit doublet accompanied by higher-energy states which comprise the satellite structure. A Lorentzian lifetime broadening $\Gamma_0=1.3-1.4$ eV was used to match the main peaks with the experimental data. For higher-energy states, a virtual-bound-state-type broadening[32] was also included to simulate the greater lifetime broadening of the higher-energy states as well as the core hole *d*-electron multiplet splitting. Such broadening has also been used to describe the 4*f* spectra of rare-earth compounds.[32] Thus the satellite peaks were broadened by an additional factor proportional to their energy separation from the main peak ΔE, such that the Lorentzian full width at half maximum (FWHM)

$$2\Gamma_n=2\Gamma_0(1+\alpha\,\Delta E)\,, \tag{5}$$

where Γ_n is the lifetime broadening of the satellite peak,

TABLE III. Best-fit parameter values (in eV) for calculated high-spin d^5 $LaFeO_3$ and d^4 $SrFeO_3$ spectra. Error bars are typically ±0.1 eV for T_σ ($\approx-2T_\pi$) and ±0.7 eV for U and Δ.

Compound	Parameters					
	Δ	T_σ	U	Q	Δ_{eff}[a]	U_{eff}[a]
$SrFeO_3$	0.0	2.2	7.8	9.4	−3.1	7.0
$LaFeO_3$	2.5	2.4	7.5	9.0	5.3	13.6
Fe_2O_3	3.5	2.4	7.0	8.4	6.3	12.7

[a]Δ_{eff} and U_{eff} are defined with respect to the lowest multiplet level of each configuration, whereas Δ and U are defined with respect to the center of gravity of each configuration (see Fig. 6).

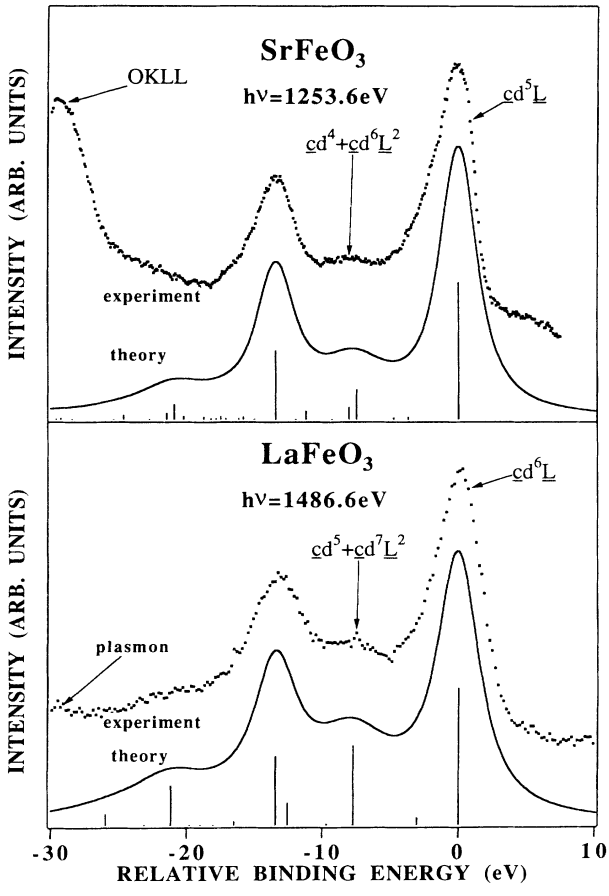

FIG. 5. Theoretical 2*p* core-level XPS spectra for $SrFeO_3$ and $LaFeO_3$ compared with experimental data after background subtraction. The experimental spectrum for $LaFeO_3$ was obtained using Al $K\alpha$ radiation (1486.6 eV) to avoid the appearance of the O *KLL* Auger emission. Best-fit parameters are displayed in Table III. Peak assignments for the calculated spectra are indicated in the figure, where $\underline{L}$ indicates a ligand hole.

and α is an arbitrary constant. ($\alpha=0.12$ and $\Gamma_0=1.4$ eV for $SrFeO_3$; $\alpha=0.15$ and $\Gamma_0=1.6$ eV for $LaFeO_3$.) A Gaussian broadening of 1.4 eV (FWHM) was then used for the entire spectrum to simulate the instrumental resolution and broadening due to the core hole-$3d$ multiplet coupling.

For $LaFeO_3$, the main peak arises from screened $\underline{c}d^6\underline{L}$ states, whereas the satellite is due to heavily mixed $\underline{c}d^5$ and $\underline{c}d^7\underline{L}^2$ states. It was found that the most dominant configuration of the satellite feature alternated between these states on small changes of Δ, although the photoemission intensity arises from the $\underline{c}d^5$ component. This result is consistent with that proposed previously for Fe_2O_3,[15] where a smaller basis was used (only d^5 and $d^6\underline{L}$). Higher-energy states due to $\underline{c}d^8\underline{L}^3$, $\underline{c}d^9\underline{L}^4$, and $\underline{c}d^{10}\underline{L}^5$ configurations appeared with negligible intensity.

Similarly, the spectrum for $SrFeO_3$ was primarily composed of main peaks due to screened $\underline{c}d^5\underline{L}$ states, and satellite structure from mixed $\underline{c}d^4$ and $\underline{c}d^6\underline{L}^2$ states. The calculated spectrum shows that a sizable, though broadened contribution from these satellite states is still present for $SrFeO_3$, even though the satellite structure seems weakened in the experimental data. For this spectrum, a parameter value of $\Delta\approx 0$ eV was used, reflecting the greater covalency of the Fe $3d$–O $2p$ states in the tetravalent compound. A vanishing or small ligand-to-metal charge-transfer energy means charge will be transferred via Fe—O bonds to the metal d orbitals from the O $2p$ bands. In fact, the cluster calculation by Adachi and Takano[27] has shown that the large covalency results in a significant loss of charge from the ionic sites. Thus the ground state of $SrFeO_3$ is unlikely to remain purely d^4, but is more likely to consist of heavily mixed d^4 and $d^5\underline{L}$ states. Further, if we take into account the multiplet splitting of the d^4 and $d^5\underline{L}$ states, the charge-transfer energy between the lowest multiplet levels, Δ_{eff}, is negative: $\Delta_{\text{eff}}=\Delta-[(4/9)(u-u')+(20/9)j]\approx -3.1$ eV (see Fig. 6), meaning that the ground state is indeed dominated by $d^5\underline{L}$ rather than d^4 configuration. This conclusion is supported by the recent Fe $2p$ x-ray-absorption study by Abbate *et al.*,[33] in which the spectrum of $SrFeO_3$ does not show the $2p^63d^4\rightarrow 2p^53d^5$ multiplet structure expected for the d^4 ionic ground state.

The Δ value for $SrFeO_3$ also follows a trend found for lower valence Fe oxides, where Δ falls by ≈ 3 eV on a change to a higher valence state, reflecting the greater covalency, i.e., for $Fe^{2+}O$, $\Delta=6$–7 eV;[31,34] for $Fe_2^{3+}O_3$, $\Delta=2.5$–3.5 eV;[15,31] for $LaFeO_3$, $\Delta\approx 2.5$ eV; and for $SrFe^{4+}O_3$, $\Delta\approx 0$ eV. The overlap integral T changes little from the trivalent case, but it was necessary to increase the value of U by a small amount in order to obtain the best fit. The reason for this is that the Fe $3d$ atomic wave function shrinks with increasing positive charges on the Fe ion, leading to a larger on-site Coulomb energy.

The occurrence of metallic behavior in $SrFeO_3$ can be examined by considering the small charge-transfer energy Δ and the large exchange stabilization of the ${}^6A_{1g}$ multiplet of the d^5 configuration as shown in Fig. 6. The large exchange stabilization of the d^5 configuration leads to a significantly larger multiplet splitting than for d^6 and d^4,

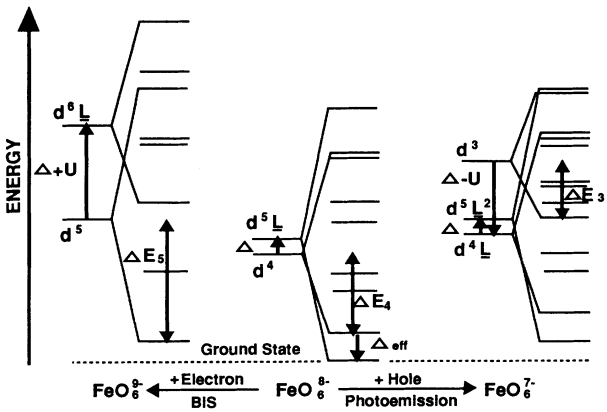

FIG. 6. Schematic energy-level diagram for the $(Fe^{4+}O_6)^{8-}$ cluster representing the hybridized ground-state configurations and excitations within the cluster. Δ is the charge-transfer energy defined with respect to the centers of gravity of the d^4 and $d^5\underline{L}$ multiplets, and Δ_{eff} is that defined with respect to the lowest multiplet levels. ΔE_n is the difference between the lowest multiplet level of the d^n configuration and its center of gravity. The large exchange stabilization of the d^5 configuration pushes down the lowest multiplet component of this configuration. Thus the band-gap energy is small and an itinerant state is likely for the d^4 configuration.

pushing down the lowest multiplet level relative to the adjacent configurations. Thus, for the d^5 system, the energy required to remove (d^5+ hole $\rightarrow d^5\underline{L}$) or add ($d^5+e^-\rightarrow d^6$) an electron to this system is large, and the localized state is stabilized. For the d^4 system, however, the energy required to add an electron ($d^4+e^-\rightarrow d^5$) is lowered, which tends to destabilize the localized state. The band gap of $SrFeO_3$ will then be of a p-p type rather than of the well-known charge-transfer type because of the negative Δ_{eff} value and the consequent $d^5\underline{L}$-like ground state. The band-gap energy for the d^5 and d^4 systems in the cluster model is

$$E_{\text{gap}}=E_{n+1}+E_{n-1}-2E_n \quad (n=4,5)\,, \tag{6}$$

where E_n is the lowest state energy of the hybridized d^n system, and was simply calculated by finding the lowest eigenenergies of the hybridized d^6, d^5, d^4, and d^3 systems. [Note, this E_n should not be confused with the center of gravity of the d^n multiplet, $E(d^n)$ used earlier.] Thus we find that E_{gap} drops from ≈ 5.5 eV for $LaFeO_3$ ($d^5+d^5\rightarrow d^6+d^5\underline{L}$) to only ≈ 0.2 eV for $SrFeO_3$ ($d^4+d^4\rightarrow d^5+d^4\underline{L}$). Considering the finite width of the ($d^4+e^-\rightarrow d^5$) and (d^4+ hole $\rightarrow d^4\underline{L}$) bands, this small E_{gap} may well lead to a vanishing band gap resulting in metallic conductivity in $SrFeO_3$ and the charge disproportionation found to occur in semiconducting $CaFeO_3$.[13] As it is the e_g electrons that are transferred in the charge fluctuation process for the d^4 system, the itinerant electrons in $SrFeO_3$ have e_g symmetry. This may correspond to the one-electron picture where metallic electrons are accommodated in an Fe $3d$–O $2p$ σ^* band, although it

must be remembered that electron correlation will be of primary importance in the metallic state, as evidenced by the local moment magnetic behavior above T_N. The charge fluctuation may also suppress the Jahn-Teller distortion of the d^4 ion, stabilizing the cubic structure down to low temperatures.

Figure 7 shows the O 1*s* core levels for Fe_2O_3, $LaFeO_3$, and $SrFeO_3$. The O 1*s* level of $YFeO_3$ was similar to that of $LaFeO_3$. As in the case of the Fe 2*p* core level, a rigid ≈ 2 eV shift is observed for Fe_2O_3, and a smaller shift of ≈ 0.5 eV to lower binding energies is seen between $LaFeO_3$ and $SrFeO_3$. One possibility for this negative shift might be the effects of screening conduction electrons which are present in metallic $SrFeO_3$ but not in insulating $LaFeO_3$.

The difference between the binding energies of the Fe 2*p* and O 1*s* core levels can be used as a measure of the chemical shift. Comparison of these difference values avoids complications due to rigid shifts of the spectra dependent on the position of the Fermi level and charging effects. From the binding energies tabulated in Table I for Fe^{2+} (Fe_xO) and Fe^{3+} (Fe_2O_3 and $LaFeO_3$), we note there is a ≈ 2 eV chemical shift to higher binding energy on the change in valence state, reflecting the large increase in charge at the Fe site. However, a much smaller chemical shift of only ≈ 0.5 eV is noted between the Fe^{3+} and Fe^{4+} ($SrFeO_3$). This is indicative of the high degree of covalency in $SrFeO_3$ which leads to a ground state of heavily mixed d^4 and $d^5\underline{L}$ character or even a ground state dominated by $d^5\underline{L}$ character. Charge transfer from the ligand sites will greatly reduce the charge on the metal, reducing the chemical shift.

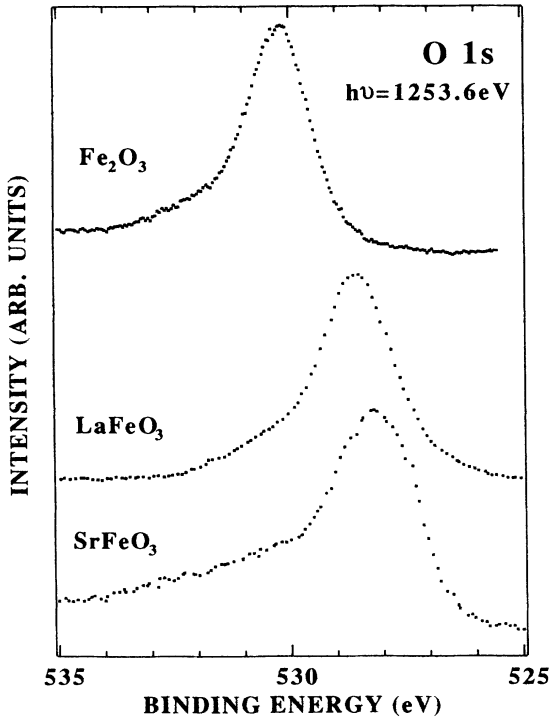

FIG. 7. O 1*s* core-level XPS spectra for Fe_2O_3, $LaFeO_3$, and $SrFeO_3$.

C. Valence band

The valence-band regions for Fe_2O_3 and $SrFeO_3$, measured by XPS (1253.6 eV) and UPS (40.8 eV), are displayed in Fig. 8. The peak located at 0–7 eV arises from the hybridized Fe 3*d*–O 2*p* bands. For $SrFeO_3$, the increase in the cross section of the O 2*p* levels for the UPS spectrum, compared to the XPS spectrum,[35] indicates that Fe 3*d*-related features are located nearer the Fermi edge and the O 2*p* band is located ≈ 5 eV below the Fermi level. The feature in the UPS spectrum located at 7–9 eV may arise from residual contamination on the surface or in grain boundaries. In analogy with other highly correlated metallic systems, such as the high-T_c superconducting copper oxides, strong correlation effects also cause the appearance of satellite features. Fujimori *et al.*[15] have used a configuration-interaction cluster calculation to predict the structure of the Fe 3*d*-derived emission in the valence region of d^5 Fe_2O_3. It was found

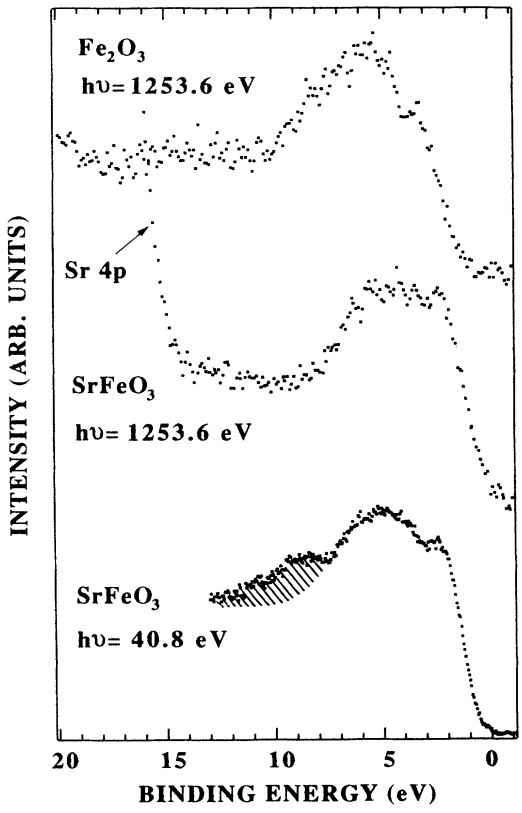

FIG. 8. Valence-band regions measured by XPS (Mg $K\alpha$: 1253.6 eV) for Fe_2O_3 and $SrFeO_3$ and by UPS (He II: 40.8 eV) for $SrFeO_3$. Following trends found for Fe_2O_3 (Ref. 15) and for the Fe 2*p* core levels, it is proposed that the main band of $SrFeO_3$ is due to $d^5\underline{L}^2$-like screened states while the broad satellite intensity at 12–13 eV is mixed $d^4\underline{L}$ and d^3 states. The feature in the UPS spectrum located at 7–9 eV (shaded) may arise from contamination on the surface or in grain boundaries.

that the main band arises from screened $d^5\underline{L}$ final states, while the satellite located at ≈ 14 eV arises from poorly screened d^4 final states. In d^4 $SrFeO_3$, on the other hand, it is proposed that the main band, and particularly the peak at ≈ 2 eV, is $d^5\underline{L}^2$-like, while the broad satellite intensity, located around 12–15 eV, is assigned to heavily mixed d^3 and $d^4\underline{L}$ states following the assignment of the Fe $2p$ core levels (Fig. 5). As in the Fe $2p$ core levels, the satellites in the $SrFeO_3$ valence region appear flatter and broader than those for Fe_2O_3. (We note here that the main peak of the Fe $2p$ core-level XPS in $SrFeO_3$ is assigned to $\underline{c}d^5\underline{L}$ rather than $\underline{c}d^6\underline{L}^2$ because of the exchange stabilization of the d^5 configuration.)

In the calculation for Fe_2O_3, structure arising from $^5T_2$ and ^5E symmetry peaks at ≈ 3 eV due to the half-filling of the t_{2g} and e_g bands, respectively, was found at the top of the valence band. In $SrFeO_3$, the e_g band is only one quarter filled and the emission is considerably weaker. Although a small step close to the Fermi edge is observed in the UPS spectrum, it cannot be seen above the background noise in the XPS measurement.

IV. CONCLUSIONS

We have studied the electronic structure of $SrFeO_3$ and shown that the ground state consists of heavily mixed d^4 and $d^5\underline{L}$ states. Analysis of the Fe $3s$ core levels, and a subsequent cluster configuration-interaction calculation, show that strong hybridization with a high-spin $d^5\underline{L}$ configuration is the key to understanding the stabilization of the high-spin $t_{2g}^3e_g$ configuration in the ground state with a small Δ. The Fe $2p$ core-level spectrum has been successfully modeled using a p-d charge-transfer cluster-type calculation which includes d-d exchange and anisotropic hybridization effects. A small or even negative charge-transfer energy, $\Delta \approx 0$ eV or $\Delta_{\text{eff}} \approx -3$ eV, means that a large amount of charge will move from the O $2p$ bands to the metal orbitals and that the ground state of the formally Fe^{4+} state is dominated by $d^5\underline{L}$ configuration rather than d^4. This charge transfer gives rise to a much reduced chemical shift between Fe^{3+} $LaFeO_3$ and Fe^{4+} $SrFeO_3$. The itinerant nature of the d electrons in $SrFeO_3$ is related to the small band-gap energy E_{gap} calculated using the cluster model for the d^4 high-spin ground state, resulting from the small Δ and the large exchange stabilization of the d^5 configuration which pushes down the adjacent d^5 levels. This small E_{gap} also leads to the charge disproportionation found to occur in $CaFeO_3$.

ACKNOWLEDGMENTS

The authors would like to thank Professor J. C. Fuggle for valuable discussions. We also thank Y. Saito and Y. Mori for helping with data acquisition, and Dr. M. Saeki for supplying the Fe_2O_3 single crystal. This work is supported by a Grant-in-Aid for Scientific Research from the Ministry of Education, Science and Culture. One of us (A.E.B.) also gratefully acknowledges the partial support by the Ministry of Education, Science, and Culture.

*Present address: Department of Physics, La Trobe University, Bundoora, VIC 3083, Australia.
†Author to whom correspondence should be addressed.

[1]See, e.g., W. E. Pickett, Rev. Mod. Phys. **61**, 443 (1989).
[2]J. Zaanen, G. A. Sawatzky, and J. W. Allen, Phys. Rev. Lett. **55**, 418 (1985); J. Zaanen and G. A. Sawatzky, Can. J. Phys. **65**, 1262 (1987); J. Solid State Chem. **88**, 8 (1990).
[3]A. Fujimori, N. Kimizuka, T. Akahane, T. Chiba, S. Kimura, F. Minami, K. Siratori, M. Taniguchi, S. Ogawa, and S. Suga, Phys. Rev. B **42**, 7580 (1990).
[4]A. Fujimori and F. Minami, Phys. Rev. B **30**, 957 (1984).
[5]Z.-X. Shen, J. W. Allen, P. A. P. Lindberg, D. S. Dessau, B. O. Wells, A. Borg, W. Ellis, J. S. Kong, S.-J. Oh, I. Lindau, and W. E. Spicer, Phys Rev. B **42**, 1817 (1990); J. van Elp, J. L. Wieland, H. Eskes, P. Kuiper, G. A. Sawatzky, F. M. F. de Groot, and J. S. Turner, Phys. Rev. B (to be published).
[6]D. J. Lam, B. W. Veal, and D. E. Ellis, Phys. Rev. B **22**, 5730 (1980).
[7]J. P. Kemp, D. J. Beal, and P. A. Cox, J. Solid State Chem. **86** 50 (1990).
[8]J. B. MacChesney, P. K. Gallagher, and D. N. E. Buchanan, J. Chem. Phys. **43**, 1907 (1965).
[9]T. Takeda, S. Komura, and N. Watanabe, in *Ferrites, Proceedings of the International Conference, Japan, 1980,* edited by H. Watanabe, S. Iida, and M. Sugimoto (Center for Academic Publication, Japan, 1981), p. 385.
[10]T. Takeda, Y. Yamaguchi, and H. Watanabe, J. Phys. Soc. Jpn. **33**, 967 (1972).
[11]T. Takeda, S. Komura, and H. Fujii, J. Magn. Magn. Mater. **31-34**, 797 (1983).
[12]M. Takano and Y. Takeda, Bull. Inst. Chem. Res. Kyoto Univ. **61**, 406 (1983).
[13]M. Takano, N. Nakanishi, Y. Takeda, and S. Naka, Mater. Res. Bull. **12**, 923 (1977).
[14]M. Takano, T. Okita, N. Nakayama, Y. Bando, Y. Takeda, O. Yamamoto, and J. B. Goodenough, J. Solid State Chem. **73**, 140 (1988).
[15]A. Fujimori, M. Saeki, N. Kimizuka, M. Taniguchi, and S. Suga, Phys. Rev. B **34**, 7318 (1986).
[16]*Handbook of X-ray Photoelectron Spectroscopy,* edited by G. E. Mullenburg (Perkin-Elmer, Eden Prairie, MN, 1979).
[17]H. Van Doveren and J. A. T. Verhoeven, J. Electron. Spectrosc. Relat. Phenom. **21**, 265 (1980).
[18]C. R. Brundle, T. J. Chaung, and K. Wandelt, Surf. Sci. **68**, 459 (1977).
[19]H. Oda, Y. Yamaguchi, H. Takei, and H. Watanabe, J. Phys. Soc. Jpn. **42**, 101 (1977).
[20]P. S. Bagus, A. J. Freemans, and F. Sasaki, Phys. Rev. Lett. **30**, 850 (1973).
[21]F. U. Hillebrecht, R. Jungblut, and E. Kisker, Phys. Rev. Lett. **65**, 2450 (1990).
[22]J. F. van Acker, Z. M. Stadnik, J. C. Fuggle, H. J. W. M. Hoekstra, K. H. J. Buschow, and G. Stroink, Phys. Rev. B **37**, 6827 (1988).
[23]S. Sugano, Y. Tanabe, and H. Kanimura, *Multiplets of Transition-Metal Ions in Crystals* (Academic, New York, 1970).
[24]B. H. Brandow, Adv. Phys. **26**, 651 (1977); J. Kanamori,

Prog. Theor. Phys. **30**, 275 (1963).
[25]Y. Tanabe and S. Sugano, J. Phys. Soc. Jpn. **9**, 766 (1954).
[26]S. Sugano and R. G. Shulman, Phys. Rev. **130**, 517 (1963).
[27]H. Adachi and M. Takano, J. Solid State Chem. (to be published).
[28]B. W. Veal and A. P. Paulikas, Phys. Rev. Lett. **51**, 1995 (1983); Phys. Rev. B **31**, 5399 (1985).
[29]J. Park, S. Ryu, M.-S. Han, and S.-J. Oh, Phys. Rev. B **37**, 10 867 (1988); J. Zaanen, C. Westra, and G. A. Sawatzky, Phys. Rev. B **33**, 8060 (1986).
[30]G. van der Laan, C. Westra, C. Haas, and G. A. Sawatzky, Phys. Rev. B **23**, 4369 (1981).
[31]A. E. Bocquet, T. Mizokawa, T. Saitoh, H. Namatame, and A. Fujimori (unpublished).
[32]J. C. Fuggle, O. Gunnarsson, G. A. Sawatzky, and K. Schönhammer, Phys. Rev. B **37**, 1103 (1988).
[33]M. Abbate, F. M. F. de Groot, J. C. Fuggle, A. Fujimori, O. Strebel, F. Lopez, M. Domke, G. Kaindl, B. T. Thole, G. A. Sawatzky, M. Takano, Y. Takeda, H. Eisaki, and S. Uchida (unpublished).
[34]This value is interpolated from those found for MnO (Ref. 3) and NiO (Ref. 4).
[35]J. J. Yeh and I. Lindau, At. Data Nucl. Data Tables **32**, 1 (1985).